Graphical abstract

Interaction Forces Between Particles Stabilized by a Hydrophobically Modified Inulin Surfactant

Jérémie Nestor, Jordi Esquena, Conxita Solans, Paul F. Luckham, Michael Musoke, Bart Levecke, Karl Booten, and Tharwat F. Tadros

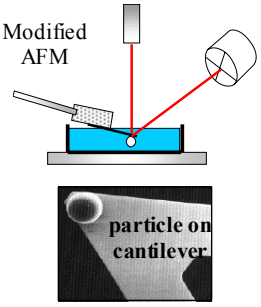

Interaction forces as a function of separation distance, at different electrolyte concentrations

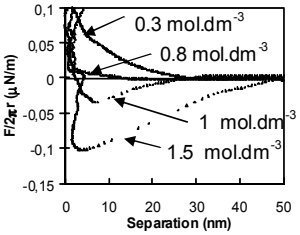

Interaction Forces Between Particles Stabilized by a Hydrophobically Modified Inulin Surfactant

Jérémie Nestor [a], Jordi Esquena [a,], Conxita Solans [a], Paul F. Luckham [b], Michael Musoke [b], Bart Levecke [c], Karl Booten [c] and Tharwat F. Tadros [d].*

[a] Departament de Tecnologia de Tensioactius. Institut d'Investigacions Químiques i Ambientals de Barcelona (IIQAB). CSIC. Jordi Girona 18-26, 08034 Barcelona, Spain.

[b] Department of Chemical Engineering and Chemical Technology, Imperial College of Science, Technology and Medicine, Prince Consort Road, London SW7 2BY, UK.

[c] ORAFTI Bio Based Chemicals, Aandorenstraat 1, B-3300 Tienen, Belgium.

[d] 89 Nash Grove Lane, Wokingham, Berkshire, RG40 4HE, UK.

*Corresponding author. E-mail: jemqci@iiqab.csic.es

Abstract

The adsorption isotherm of a hydrophobically modified inulin (INUTEC SP1) on Polystyrene (PS) and Poly(methyl methacrylate) (PMMA) particles was determined. The results show a high affinity isotherm for both particles as expected for a polymeric surfactant adsorption. The interactions forces between two layers of the hydrophobically modified inulin surfactant adsorbed onto a glass sphere and plate was determined using a modified atomic force microscope (AFM) apparatus. In the absence of any polymer, the interaction was attractive although the energy of interaction was lower than predicted by the van der Waals forces. The results between two layers of the adsorbed polymer confirms the adsorption isotherms results and provides an explanation to the high stability of the particles covered by INUTEC SP1 at high electrolyte concentration. Stability of dispersions against strong flocculation could be attributed to the conformation of the polymeric surfactant at the solid/liquid interface (multipoint attachment with several loops) which remains efficient at Na_2SO_4 concentration reaching 1.5 $mol.dm^{-3}$. The thickness of the adsorbed polymer layer in water determined both by AFM and rheology measurements, was found to be about 9 nm.

1. Introduction

Polymeric surfactants are commonly used in formulations that require high colloid stability, such as paints, cosmetics products, emulsion latexes, etc [1]. The mains advantages of polymeric surfactants are their strong adsorption at the solid/liquid interface (lack of desorption) due to the multipoint attachment of the polymer chain to the surface and the strong steric repulsion between the stabilizing chains. This can be achieved using block or grafted copolymers, where the B part of the molecule acts to anchor the chain to the surface, and the A part is the stabilization chain [2-5]. The performance of a polymer depends not only upon its adsorption density but also on its conformation and orientation at the interface. For an adsorbing polymer system, the balance of interaction energies between the polymer and solvent, the polymer and surface, and the polymer with itself will determine the final conformation adopted at the interface [6]. It is essential to have an adsorbed layer thickness that is sufficiently large to screen the Van der Waals attractive forces [7].

To achieve the above objective, a hydrophobically modified inulin surfactant (INUTEC SP1) has been recently synthesized [8-9]. This molecule is a graft copolymer consisting of an Inulin (Polyfructose) backbone (A) on which several alkyl groups (C_{12}) (B) are grafted. The inulin backbone has a degree of polymerization greater than 23 (i.e. a molecular weight greater than 3700 dalton).

The alkyl groups provide the anchor points (multipoint attachment) at the solid/liquid interface, leaving the polyfructose loops dangling in solution. These alkyl chains are randomly distributed across the polyfructose backbone which implies a distribution of loop sizes. The polyfructose chain remains strongly hydrated even at high electrolyte concentration and high temperature [10-11]. The molecule was previously studied for his stabilization properties of O/W emulsions [11] and colloidal dispersions such as latex particles [12-13]. Preliminary investigations by dynamic light scattering (PCS) using polystyrene latex particles, indicated an adsorbed polymer layer thickness of 4 nm [12]. It proved to be very effective as a steric stabilizer [12,13] and indeed more

efficient in comparison to classical surfactants, based on poly(ethylene oxide) [12-15].

For full characterisation of an adsorbed polymer layer, at a solid/liquid interface, one needs to know how much polymer is absorbed, where it is located on the surface, and how far it extends into solution away from the interface (the hydrodynamic layer thickness). Polymer adsorption has traditionally been studied quantitatively by classical solution depletion. More recently, the adsorbed polymer layer has been investigated by rheology [16] and by direct force measurements such as atomic force microscopy (AFM) [17]. Both techniques provide information about the adsorbed layer thickness as a function of polymer concentrations.

In this paper, we report the results of a study of the mechanism of stabilization of solid particles by the INUTEC SP1. The adsorption of INUTEC SP1 on PS and PMMA particles has been investigated. The polymer coated latex particles were used for rheological investigations as a function of the volume fraction of the particles. To fully understand the stabilization mechanism, a quantitative description of the interaction forces between the adsorbed polymer layers was obtained using AFM measurements. For this purpose, the interaction between a hydrophobized glass sphere and a glass plate, that were coated with Inutec SP1, was measured as a function of polymer concentration, both in aqueous solution and in the presence of Na_2SO_4 (up to 1.5 mol.dm^{-1}).

2. Experimental

2.1. Materials

INUTEC SP1 was supplied by ORAFTI Bio Based Chemicals (Tienen, Belgium), and was synthesized as described before [8-9]. It is a graft copolymer made of a polyfructose backbone on which some alkyl groups (C_{12}) are grafted. Its average molecular weight is approximately 5000 $g.mol^{-1}$. The purity of such surfactant was higher than 97% and it forms a clear solution at concentrations less than 0.1 wt%, above which a turbid solution appears which is due to some association of the polymeric chains [13].

Styrene (Merck) or Methyl Methacrylate (Aldrich) were used as monomers. These were purified by passing them through basic chromatographic aluminum oxide in order to remove the hydroquinone inhibitor. Potassium persulfate, $K_2S_2O_8$, was obtained from Fluka with purity higher than 99%. Deionized water was further purified by filtration through a milli-Q system. The electrolytes used were calcium chloride, $CaCl_2$. $2H_2O$ (purity > 99%) supplied by SIGMA and sodium sulphate, Na_2SO_4 (purity > 99%) supplied by BDH. For the AFM experiments, the water used was filtered through a Nanopure system (water resistance >10 MΩ, surface tension =72 ±0.2 $mN.m^{-1}$).

2.2. Methods

Latex particles

All latexes were prepared by emulsion polymerization as described before [13]. The reactions were carried out for 24 hours for polystyrene (PS) particles and 6 hours for poly(methyl methacrylate) (PMMA) particles, at a constant temperature of 80ºC under a controlled nitrogen atmosphere.

A complete characterization of both latexes was carried out. The main results, such as diameter, polydispersity index, conversion rate, and the critical coagulation concentrations (CCC) of $CaCl_2$, are shown in Table 1. The monomer conversion rates were determined at the end of the reaction, for each latex synthesized, by the gravimetric method based on evaporation of all volatile compounds of the dispersion, at 50ºC during 12 hours. Particle size and

polydispersity index of each particle were obtained by photon correlation spectroscopy, PCS. The CCCs were evaluated by measuring the turbidity as a function of time for different electrolyte concentrations. Details of the method have been reported elsewhere [13].

AFM experiments

The atomic force microscope (AFM) used was constructed at the Imperial College with the specific aim of examining the surface interactions between adsorbed polymer layers on glass surfaces. No scanning capability was incorporated into the instrument. A full description of the instrument and its operation was given elsewhere [18]. To minimize the drifts and noise from both the environment and the mechanical apparatus itself, the apparatus was set up in a basement laboratory, placed on an antivibration table and covered with a custom-made box to control the local environment.

The glass surfaces (30 ml Petri dish with flat bottom and glass spheres of about 30 μm diameters) were rigorously cleaned by ultrasonication in dilute RBS 50 detergent solution (Chemical Concentrates, Ltd.) and then rinsed thoroughly with water and dried under a laminar flow hood in a special clean room to avoid dust contamination.

To prepare hydrophobic surfaces, the glass spheres and Petri dishes were immersed in a mixture of 5 wt% solution of dichlorodimethylsilane (BDH) in 1,1,2-trichloroethylene at 75 ºC for 24 hours in a vacuum oven. The hydrophobicity of the surface was checked by observing the contact angle of water on the flat glass surface. In all cases, the contact angle of water was approximately near to 180º, indicating a hydrophobic surface.

The glass sphere was mounted onto a commercial silicon AFM single beam cantilever using a micromanipulator and video camera. The particle diameter was determined microscopically and the spring constant of the lever was determined using the resonance shift technique similar to the one described by Cleveland [19]. The spring constant can be expressed by the expression:

$$k = \frac{4\pi \upsilon_L^2 \upsilon_u^2 m_p}{\left(\upsilon_u^2 - \upsilon_L^2\right)} \qquad (1)$$

where ν_u and ν_L represent the resonance frequencies of the cantilever while unloaded and loaded respectively and m_p, is the particle mass. A spring constant of 0.0147 $N.m^{-1}$ was determined for the cantilevers used in our experiments.

The Petri dish was mounted on top of the AFM moving vertical stage and filled with nanopure water (30 ml). The two surfaces were brought into close proximity of roughly 2 mm apart after which a part of the nanopure water was replaced by some stock polymer solution using a hypodermic needle to obtain the adequate polymer concentration in the bulk. The surfaces were then left at least 12 hours to allow the polymer to adsorb on the silanized surfaces. The raw data were collected using a commercial software package called Snapshot (Advantech, UK), and finally the data were processed in commercially available spreadsheet software (Excel 2000). All experiments were carried out at room temperature.

Adsorption Isotherms

The adsorption isotherms were determined by using the depletion method [20], which consists of measuring the difference between the surfactant concentration in solution before and after adsorption. Surfactant adsorption was performed for 12 hours at 25 ± 0.1ºC by adding different amounts of surfactant to latex particles with 0.3 m^2 of overall area. The surfactant-latex mixtures were gently shaken during and after the addition of surfactant. The latexes were separated by centrifugation for 15 minutes at 15000 rpm. The concentration of surfactant in solution was determined by a colorimetric method based on the reaction between fructose and thiobarbituric acid [21]. Surfactant solutions were mixed with thiobarbituric acid (2,883 $g.dm^{-3}$ solution), in the presence of $HCl_{(aq.)}$,1 $mol.dm^{-3}$, placed in a boiling bath for 6 minutes, and the absorbance measured by spectrophotometry at 430 nm. This method was adapted to

measure low concentration of INUTEC SP1. The adsorbance vs. concentration curve was linear in the range 2.10^{-6} mol.dm^{-3} up to $1.2.10^{-4}$ mol.dm^{-3}.

Rheological measurements

The rheological measurements were performed at 25 ºC using a HAAKE 150 Rheometer equipped with double cone geometry. The temperature control was achieved to within ± 0.2ºC. The latex dispersion was carefully placed in the gap between the double cone geometry and the plate. The double cone was rotated at various angular velocities enabling the shear rate, $\dot{\gamma}$, to be estimated, the torque and hence the stress was measured on the other element.

The rheology of aqueous PS particles sterically stabilized by post-addition of INUTEC has been studied. In order to have a high rate of adsorption of the polymer, particles dispersions were mixed with polymer solution for 24 h, to allow the polymer to adsorb at the interface. Steady state measurement has been carried out for PS samples with various volume fractions, ϕ (0.1 to 0.42). All the samples had the same polydispersity since each different volume fraction sample was concentrated from the same batch of latex.

3. Results and Discussion

3.1. Adsorption isotherms

Results of adsorption of the INUTEC SP1 on PS and PMMA particles are shown in Figure 1.

In both cases, a high affinity isotherm is observed which indicates the strong adsorption of the polymer (multipoint attachment) both on the PS and PMMA particles. The shape of the adsorption isotherms suggests polydisperse polymer molecules [6].

The amount of surfactant adsorbed on PMMA particles is higher than that adsorbed on the PS particles. This may indicate a more densely packed layer on the PMMA surface. It is quite likely that the conformation of the polymer at the solid liquid interface depends on the nature of the surface [22-23]. The area per molecule at the pseudo-plateau of the isotherms is 48 nm^2 for PS particles and 34 nm^2 for PMMA particles which may indicate that the surface is not fully covered

The present data are strongly reminiscent of the two regimes described by Alexander and de Gennes for the adsorption of block copolymers [24-25]. The dilute regime with a strongly affinity for the surface was observed at low polymer concentration ($<5x10^{-4}$ $mol.dm^{-3}$) where the surface was either bare or not too much “crowded”, leading to a very strong adsorption. The semi-dilute regime at higher concentration was characterized by a lower affinity for the surface because lateral interactions occur between adsorbed polymer molecules inhibiting further adsorption. The Alexander De Gennes model is strictly for an adsorbing AB copolymer, where one part of the polymer extends away as a tail from the surface. In the present case, the hydrophobic part of the polymer is grafted to an inulin backbone so we will have a significant number of loops present as well as tails. However the same argument holds as these loops and tails will stretch away from the surface as more polymer molecules adsorb.

3.2. CCC as a function of surfactant adsorption

Figure 2 shows the effect of the adsorption of INUTEC SP1 on the stability of the PS and PMMA particles. The critical coagulation concentration (CCC), determined with $CaCl_2$, is plotted as a function of the INUTEC SP1 area per molecule, calculated from the adsorption isotherm data. As it can be seen, the stabilization is enhanced before full coverage of the PS and PMMA particle by the INUTEC SP1, at areas per molecule about 100 nm^2 in both cases. The more molecules of INUTEC are added (decrease of the area per molecules) the more stability against the coagulating action of the electrolyte is observed. Furthermore this effect seemed to increase exponentially as a function of the surfactant adsorbed. This can be explained because, as the adsorption increases, the polyfructose loops of the polymer are extended further away from the particle surface, enhancing the particle stability. The stabilization depends also on the latex surface properties since a smaller amount of INUTEC SP1 is needed to stabilize the PMMA particles than the PS particles.

These observations confirm the hypothesis that INUTEC SP1 adsorbed on the hydrophobic surface by the hydrophobic alkyl chains and hydrophilic polyfructose chains form loops dangling in solution, giving rise to an extended polymer layer and hence being able to act as an effective steric stabiliser. Stabilization appears long before the surface is saturated due to the strongly hydrated polyfructose loops. The surfactant added is filling the free gaps on the particles surface, increasing the surfactant loop density at the interface which then extends further from the particle surface.

3.3. Determination of interaction forces by AFM

3.3.1. Interaction between bares hydrophobic surfaces

To establish how the polymer modifies the interaction between two surfaces, it is first necessary to determine the interactions between bare surfaces (hydrophobic). These results are shown in Figure 3 where the force is

plotted as a function of the distance curve between glass sphere/plate probes. In the approach process, interaction begins at around 45 nm from contact. At this distance the surfaces jump spontaneously into contact. On withdrawal, a very strong attraction is observed followed by a jump out to 150 nm from the surface. Figure 3 also shows the theoretical Van der Waals attractions. These forces have been estimated assuming a Hamaker constant for glass of 10^{-20} J [26], which is likely to be an overestimate for hydrophobic glass surfaces. It is clear that the theoretical Van der Waals forces are weaker than those observed experimentally. Long range, strongly attractive interactions between two hydrophobic surfaces have been commonly reported in the literature [27-29]. The origin of such interaction are not entirely clear, but some authors attributed these forces to the presence of small air bubbles nucleated on the hydrophobic surface [30], which, when it comes in contact with another hydrophobic surface caused a bridging of the nanobubbles, drawing the two surfaces together .

The main conclusion of the above results, is that in absence of any polymer adsorbed on the surfaces, a long-range attractive interaction between the hydrophobic surfaces is observed. No further experiments were carried out to provide a more complete description of these interactions, since it is out of the scope of the present paper.

3.3.2. Effect of the polymer adsorption on the interactions between hydrophobic surfaces

Figure 4 presents the interaction between hydrophobic glass surfaces immersed in solutions of different concentrations of polymer, varying from $1x10^{-5}$ to $2x10^{-4}$ mol.dm^{-3}, the last concentration corresponding to the limit of solubility of the INUTEC. Several (at least 3) repetitions of the experiments have been performed. In most cases, agreement between the results from repeated experiments was good and within the experimental error of the experiment. For clarity, only one set of data is plotted in Figure 4.

For a concentration of $1x10^{-5}$ mol.dm^{-3} polymer in solution (Figure 4a), the interactions forces seem to be similar to these observed between two bare

hydrophobic glass surfaces. But a careful observation of Figure 4a reveals that on compression a weak and ill defined repulsion appears when surfaces are some 15 nm from contact (see insert to Fig 4a), followed by the attraction similar to those observed for the hydrophobic surfaces. This weak repulsion may be due to a small amount of the polymer adsorbed on the glass surfaces. This repulsion is certainly not sufficient to ensure a good stabilization of the particles against flocculation.

A well defined repulsive interaction is indicated on approach of the surfaces (Fig. 4b), for concentration of polymer equal to 6.6×10^{-5} mol.dm^{-3}. However on withdrawal, the interaction remains attractive, because the surface is not completely saturated and after compression, the polymer remains displaced giving rise to an attraction on separation, which is considerably weaker than in the absence of any polymer. For concentrations equal to, or greater than 1.6×10^{-4} mol.dm^{-3} (Fig. 4c and 4d) the interactions become repulsive in both approach and retraction. The repulsion is due to the steric interaction between the adsorbed polymer layers; it is a combination of the osmotic pressure due to the increase of the polymer concentration between the two surfaces on compression and a decrease in entropy of the polymer as it is compressed.

In the above two cases (Fig. 4c and 4d) the hysteresis (the small difference between the approach and the withdrawal curves) is probably due to the inaccuracy of the measurements and one cannot draw any conclusion from it. These small variations may be within the experimental error of the measurement.

The results of Fig. 4b indicate that the repulsion initiates at a separation distance of 8 nm. The use of AFM techniques to determine the layer thickness suffers from having an ambiguous point of zero distance separation [31], but it could be assumed that the layer thickness is half the separation where the repulsion between the two surfaces begins to occur. However, since in this case the repulsion disappears on withdrawal, one cannot use this value as a real thickness. The only results that may give an estimate of the layer thickness are shown in Fig. 4c and 4d, which show that the repulsion starts to be significant at a separation distance of approximately 18 nm, indicating a layer thickness of about ~9 nm. This value seems to be an overestimate considering the

molecular weight of the polyfructose backbone, which contains about 25 fructose units. It is highly unlike to obtain a loop greater than 2 nm if one does not take into account the contribution of the hydration shell.

The most likely explanation of this high layer thickness obtained is due to the polydispersity of the loop sizes and their strong hydration. One may also infer from the results of Fig. 4c and Fig. 4d that the beginning of the repulsion, at separation distance of about 9 nm, is caused by the largest hydrated loops. On further reduction of separation distance, these larger loops may become compressed and further stronger repulsion occurs between the smaller hydrated loops.

It is difficult to directly compare the AFM results to the concentration of polymer necessary to saturate the solid/liquid interface, because in one case the polymer is adsorbed on hydrophobic glass surfaces and in the other case is adsorbed on latex particles. These two kinds of surface certainly do not present quite the same hydrophobic character, and we can see that different levels of adsorption occur on polystyrene and poly(methyl methacrylate) particles. Furthermore, the adsorption conditions are very different in the two experiments, as in the AFM experiments (a few cm^2), the surface area is much smaller than in the adsorption study on latex particles (a few m^2).

3.3.3. Effect of electrolyte concentration

Presented in Figure 5 are the force profiles for the interaction between two adsorbed layers of INUTEC SP1 in presence of different electrolyte (Na_2SO_4) concentration from 0.3 to 1.5 $mol.dm^{-3}$. The concentration of INUTEC SP1 in solution has been kept at $1x10^{-4}$ $mol.dm^{-3}$ as it has been previously shown that solid/liquid interface is completely covered by the polymer at this concentration. It can be observed that on approach, the interactions remain repulsive even at high electrolyte concentration, although the electrolyte has reduced the polymer layer thickness from approximately 10 nm at 0.3 $mol.dm^{-3}$ of electrolyte, to 3 nm in presence of 1.5 $mol.dm^{-3}$ of electrolyte. This reduction in hydrodynamic thickness in the presence of high electrolyte concentration could be due to a change in the conformation of the polyfructose loops. It is highly unlikely that dehydration of the chains occurs since recent cloud point

measurements, not reported here, have shown absence of any cloud point up to 100 °C. Even at such low adsorbed layer thickness, strong repulsive interaction is observed indicating a high elastic repulsive term. This is confirmed by the lack of any attractive interaction on approach even at high electrolyte concentration. This clearly indicates that INUTEC SP1 would be an effective colloidal stabilizer in a large range of electrolyte concentration as already observed in other studies [12-13].

On withdrawal (Fig. 5b), the interaction remains repulsive up to 0.8 mol.dm^{-3} Na_2SO_4. However an attractive interaction appears for electrolyte concentration higher than 1 mol.dm^{-3}. This could be explained by a change of the conformation of the loops at the interfaces, which allows the Van der Waals forces to dominate close to the surface after compression. One has to take in account that compression of the polymer layer in the AFM experiment is much stronger than the one occurring due to the Brownian collision. Measurement of CCC Na_2SO_4 (CCC_{Na2SO4} > 1.5 mol.dm^{-3}, reported in Table 2) of PS particles confirms the high stability of particles bearing an adsorbed layer of INUTEC even at high electrolyte concentration.

Figure 6 shows a comparison between the interactions of two bares hydrophobic surfaces (silanized), and two hydrophobic glass surface covered by INUTEC SP1 immerged in concentrated electrolyte solution (1.5 mol.dm^{-3}). It can be observed that the interaction forces are only repulsive for approaching surfaces bearing INUTEC SP1 layer. On retraction, the attraction observed for the surfaces covered by INUTEC SP1 (-0.1μN.m^{-1}) are much weaker than those observed for the hydrophobic surfaces (-0.3 μN.m^{-1}). The difference in magnitude of the interaction forces between the bare hydrophobic surfaces and surfaces covered by polymers in presence of 1.5 mol.dm^{-3} Na_2SO_4 indicates the existence of a thin collapsed polymer layer on the surface, rather than the original hydrophobic surface. These results may explain the very high CCC Na_2SO_4 value obtained with PS particles stabilized by INUTEC SP1, as observed in Table 2.

3.4. Determination of the adsorbed layer thickness using rheology

As observed in Figure 4c and 4d, the statically adsorbed layer thickness of the polymer when the polyfructose loops are fully extended is about 9 nm, which is quite thick in comparison with the INUTEC SP1 molecular weight (5000 g/mol), as discussed before. This can be explained partially by a very strong hydration of the polyfructose molecules and partially to the likely polydispersity of the polymer loops. This hydration is consistent to measurements of the cloud point of the polyfructose backbone (i.e. in the absence of any hydrophobic groups) has shown an absence of any cloudiness up to 100ºC and at electrolyte concentrations reaching 2 mol.dm^{-3} Na_2SO_4.

Figure 7 shows the variation of the relative viscosity, η_r, with volume fraction, ϕ, for PS core particle dispersions with a mean diameter of 321 nm. For comparison the η_r - ϕ curves calculated using the Dougherty- Krieger [32] equations is shown on the same figure.

$$\eta_r = \left[1 - \left(\frac{\phi}{\phi_p}\right)\right]^{-[\eta]\phi_p} \qquad (2)$$

Where [η] is the intrinsic viscosity that is consider equal to 2.5 for hard sphere and ϕ_p is the maximum random packing fraction (~0.6) [33].

As it can be observed, the viscosity of all systems is higher than predicted and, the theoretical η_r - φ curve for the PS suspensions stabilized by INUTEC SP1 is shifted to the left as a result of the polymer adsorbed. The polymer layer that is adsorbed to the particle also contributes to the hydrodynamic volume of the particles. The experimental relative viscosity data could be used to obtain the effective volume fraction. The maximum packing fraction may be obtained from a plot of $1/(\eta_r)^{1/2}$ vs, ϕ and extrapolation to $1/(\eta_r)^{1/2} = 0$, using an empirical procedure described by Tadros et al. [34. The value of maximum package fraction, ϕ_p, using this method was found equal to 0.505 (which is lower than the maximum random packing fraction for hard spheres, ~ 0.6).

Using ϕ=0.505 and ϕ_{eff}=0.6, the grafted polymer layer thickness was calculated using the equation:

$$\phi_{eff} = \phi\left[1+\left(\frac{\delta}{R}\right)\right]^3 \qquad (3)$$

From this equation, a layer thickness, δ = 9.6 nm was obtained, which is consistent with the AFM results described above. It is higher than the approximate value (4 nm) obtained before, by measuring the small increase in the hydrodynamic radius of latex particles, determined from diffusion coefficients obtained by PCS, as a function of surfactant concentration [12]. The PCS measurements are less accurate since δ is obtained from the difference between the hydrodynamic radius of the polymer coated particles and the bare particles. Since δ is much smaller than the radius of the particles (less than 10 times), the accuracy of this technique is not as good as that of the AFM and the rheology.

Conclusions

AFM experiments combined with adsorption studies have allowed us to describe the structure of the adsorbed INUTEC SP1 layer. At low concentration, rapid adsorption of polymer occurs, generating a thin layer of polymer of a few nanometers thickness, with some of the polymer loops or tails dangling into solution. Increasing the polymer concentration results in full adsorption of INUTEC SP1 which becomes slower because access to the interface is more difficult due to the presence of molecules that are already adsorbed. Increasing the number of molecules adsorbed at the interface changes the conformation of the polymer such that the polyfructose loops become more extended from the surface. At even higher polymer concentration, the surfactant added is filling the gaps left on the particle surface which are few and far between, so the polyfructose layer thickness does not change significantly

The polymer layer thickness had been determined when the polymer reached its maximum extension. Results obtained by AFM and rheological measurements are consistent with a single layer of molecules, having an average layer thickness of, $\delta = 9 \pm 2$ nm. Finally, AFM measurements between surface bearing INUTEC SP1 and in presence of high electrolyte concentration show the existence of a thin layer of polymer which may explain the very high value of CCC observed on latex particles stabilized by INUTEC SP1.

Acknowledgements

The authors gratefully acknowledge financial support from ORAFTI Bio Based Chemicals and from the Spanish Ministry of Science and Education (PPQ2002-04514-C03-03 grant). We also have to acknowledge the research group offering the rheometer (Prof. J.M. Gutiérrez and Dr. A. Maestro).

References

[1] D. Myers, Surfactant Science and Technology, 2nd ed. VCH Publishers, Inc.; 1992.

[2] R.H. Ottewill, T. Walker, Kolloid Z. Z. Polym. 227 (1968) 108.

[3] R.H. Ottewill, T. Walker, J. Chem. Soc. Faraday Tran. 70 (1974) 917.

[4] Th.F. Tadros, The effects of polymers on dispersion properties. Academic Press: London, 1982.

[5] Th.F. Tadros, In Novel Surfactants; Marcel Dekker: New York, 2003.

[6] G.J. Fleer, M.A. Cohen Stuart, J.M.H.M. Scheutjens, T. Cosgrove, B. Vincent, Polymers at Interfaces; Chapman & Hall: London, 1993.

[7] R.J. Hunter, In Foundations of colloid science, Oxford University press, New York, 1986, p 454.

[8] C.V. Stevens, A. Meriggi, K. Booten, Biomacromolecules 2 (2001) 1.

[9] C.V. Stevens, A. Meriggi, M. Peristeropoulou, P.P. Christov, K. Booten, B. Levecke, A. Vandamme, N. Pittevils, Th.T. Tadros, Biomacromolecules 2 (2001) 1256.

[10] Th.F. Tadros, A. Vandamme, K. Booten, B. Levecke, C. V. Stevens, Colloids and Surfaces A. 250 (2004) 133.

[11] Th.F. Tadros, A. Vandamme, B. Levecke, K. Booten, C. V. Stevens, Adv. Colloid Interface Sci. 108 (2004) 207.

[12] J. Esquena, F.J. Dominguez, C. Solans, B. Levecke, K. Booten, Th.F. Tadros, Langmuir 25 (2003) 10463.

[13] J. Nestor, J. Esquena, C. Solans, B. Levecke, K. Booten, Th. F. Tadros, Langmuir 21 (2005) 4837.

[14] D.H. Napper, Polymeric Stabilization of Dispersions; Academic Press: London, 1983.

[15] M.B. Einarson, J. Berg, J. Colloid Interfaces Sci. 155 (1993) 165.

[16] M.A. Faers, P.F. Luckham, Colloids Surf. 86 (1994) 317.

[17] M. Musoke, P.F. Luckham, J. Colloid Interfaces Sci. 277 (2004) 62.

[18] G.J.C. Braithwaite, A. Howe, P. F. Luckham, Langmuir 12 (1996) 4224.

[19] J.P. Cleveland, S. Manne, D. Bocek, P.K. Hansma, Rev. Sci. Instruments 64 (1993) 403.

[20] A. Martín-Rodríguez, M.A. Cabrerizo-Vílchez, R.J. Hidalgo-Álvarez, Colloid Interface Sci. 187 (1997) 139.

[21] A.B. Blakeney, L. L. Mutton, J. Sci. Food Agric. 3 (1980) 889.

[22] B. Kronberg, P. Stenius, G. Igeborn, J.Colloid Interface Sci. 102 (1984) 418.

[23] A. Martín-Rodríguez, M.A. Cabrerizo-Vílchez, R. Hidalgo-Álvarez, Colloid Surf. A. 92 (1994) 113.

[24] S. Alexander, J. Phys. 38 (1977) 983.

[25] P.G. de Gennes, Macromolecules 13 (1980) 1069.

[26] J. Israelachvili, Intermolecular and Surface Forces; Academic Press: London: 1992.

[27] R.M. Pashley, P.M. McGuiggan, B.W. Ninham, Science 229 (1985) 1088.

[28] P. Attard, Langmuir 16 (2000) 4455.

[29] N. Ishida, M. Sakamoto, M. Miyahara, K. Higashitani, Langmuir 16 (2000) 5681.

[30] P. Attard, Adv. Colloid Interface Sci. 104 (2003) 75.

[31] G.J.C. Braithwaite, P.F. Luckham, J. Chem. Soc., Faraday Trans. 93 (1997) 1409.

[32] I.M. Krieger, T. J. Dougherty, Trans. Soc. Rheol. 3 (1959) 137.

[33] Th. F. Tadros, Adv. Colloid Interface Sci. 104 (2003) 191.

[34] C. Prestidge, Th.F. Tadros, J. Colloid Interface Sci. 124 (1988) 660.

Table 1. Main Features of Latexes. Particle diameter, polydispersity index (PI), monomer conversion (X), and critical coagulation concentration of $CaCl_2$ (CCC) of PS and PMMA particles.

Sample	Particle size (nm)	PI	X (%)	CCC (M)
PS	321,6	0,031	91	0,018
PMMA	273,1	0,054	94	0,024

Table 2. Variation of the critical coagulation concentration ($CCC_{Na_2SO_4}$) as a function of the INUTEC post-added on PMMA particles synthesized by surfactant-free emulsion polymerization.

[INUTEC]/[PMMA]	CCC_{Na2SO4}
0	0,54
0,005	0,86
0,008	1,24
0,01	>1,5
0,02	>1,5
0,05	>1,5
0,1	>1,5
0,5	>1,5

FIGURE LEGENDS

Figure 1: Isotherm for the adsorption of INUTEC SP1 on PS (open circles) and PMMA particles (filled circles).

Figure 2. Effect of the adsorption of INUTEC SP1 on the CCC_{CaCl2} of PS (open circles) and PMMA particles (filled circles).

Figure 3. Force distance interaction profile between hydrophobic (silanized) glasses immersed in nanopure water. Solid symbols correspond to approach, open symbols to withdrawal. The theoretical van der Waals attraction, calculated assuming a Hamaker constant equal to 10^{-20} J [26], is also shown, and compared to the approach data.

Figure 4. Force distance interaction profile between hydrophobic (silanized) glass bearing an adsorbed layer of INUTEC SP1. a) with 1.10^{-5} mol.dm^{-3} INUTEC SP1 in solution, b) with $6{,}6.10^{-5}$ mol.dm^{-3} INUTEC SP1 in solution, c) with $1{,}6.10^{-4}$ mol.dm^{-3} INUTEC SP1 in solution, d) with 2.10^{-4} mol.dm^{-3} INUTEC SP1 in solution. Solid symbols correspond to approach, open symbols to withdrawal.

Figure 5: Force distance interaction profile between hydrophobic (silanized) glass bearing an adsorbed layer of INUTEC SP1 immersed in different Na_2SO_4 concentration solution. a) Approach, b) withdrawal.

Figure 6: Comparison of force distance interaction profile between hydrophobic (silanized) glass bearing an adsorbed layer of INUTEC SP1 immerged in 1.5 mol.dm^{-3} Na_2SO_4, and Hydrophobic (silanized) glass without polymer. Solid symbols correspond to approach, open symbols to withdrawal.

Figure 7. Relative viscosity vs. volume fraction for PS suspensions with a means diameter of 321 nm. Dash line represents the theoretical curve calculated from the Dougherty- Krieger equations.

5: Figure 1

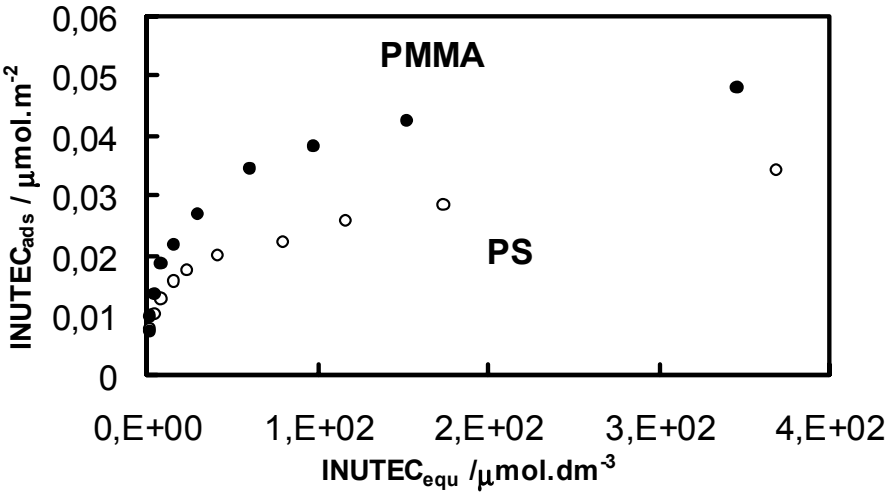

Figure 1

5: Figure 2

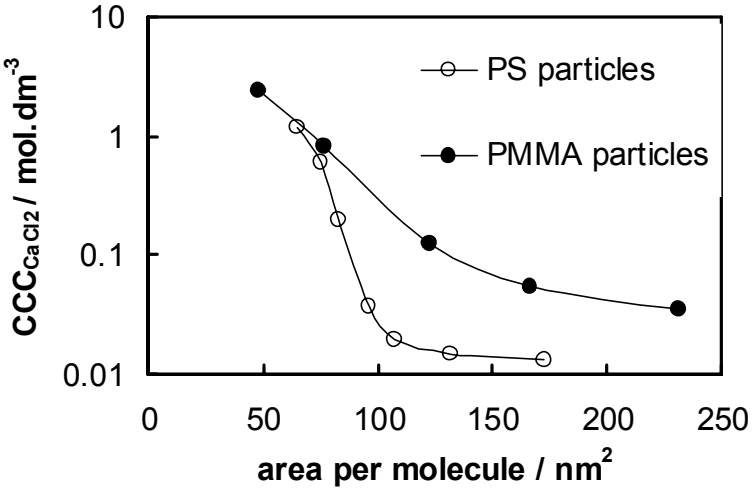

Figure 2

5: Figure 3

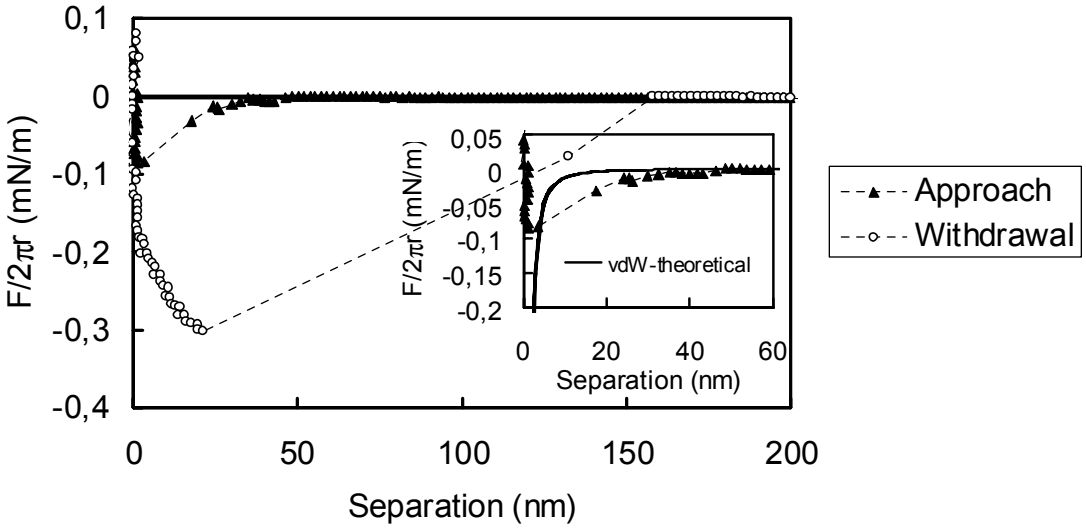

Figure 3

5: Figure 4

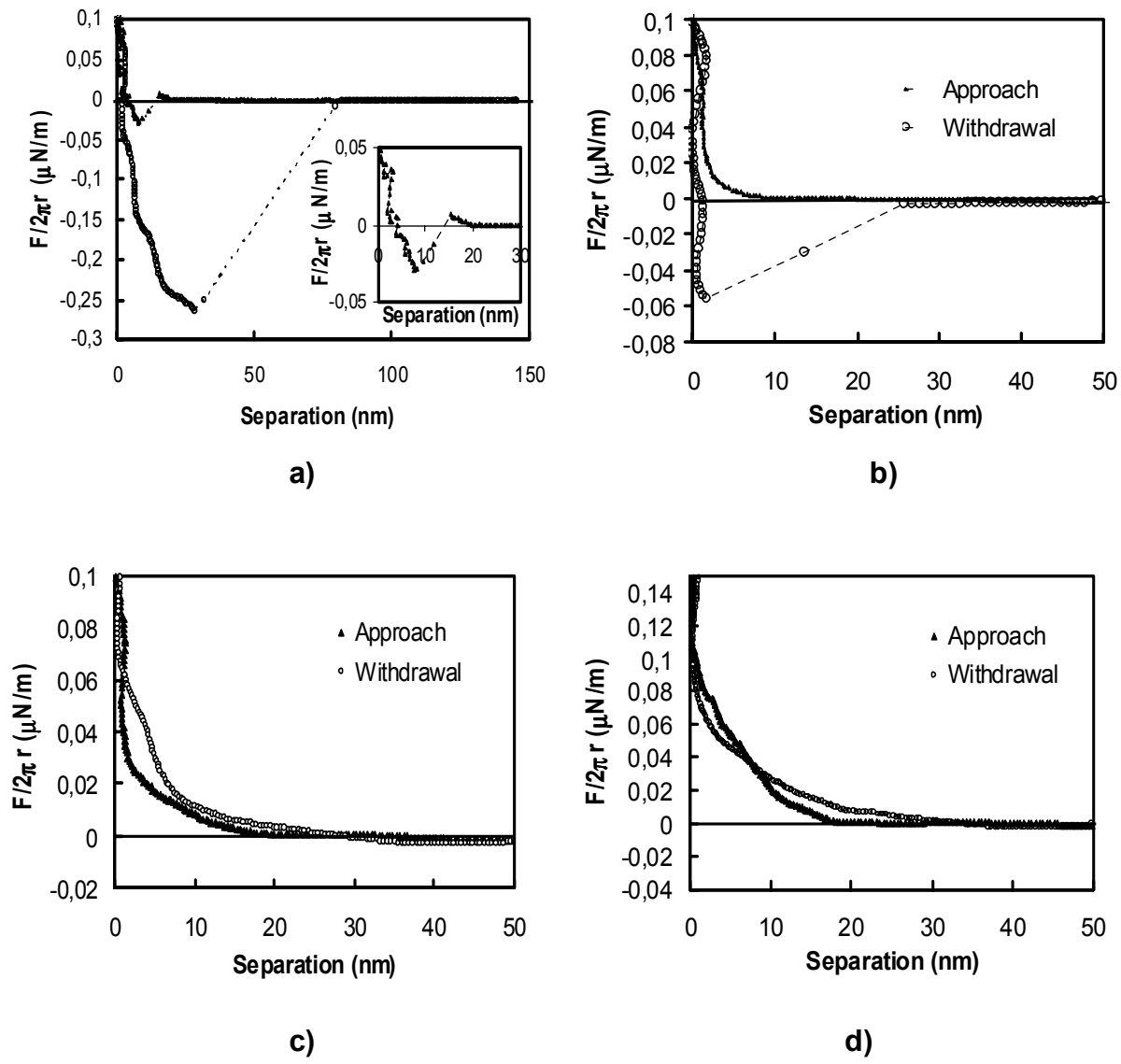

Figure 4

5: Figure 5

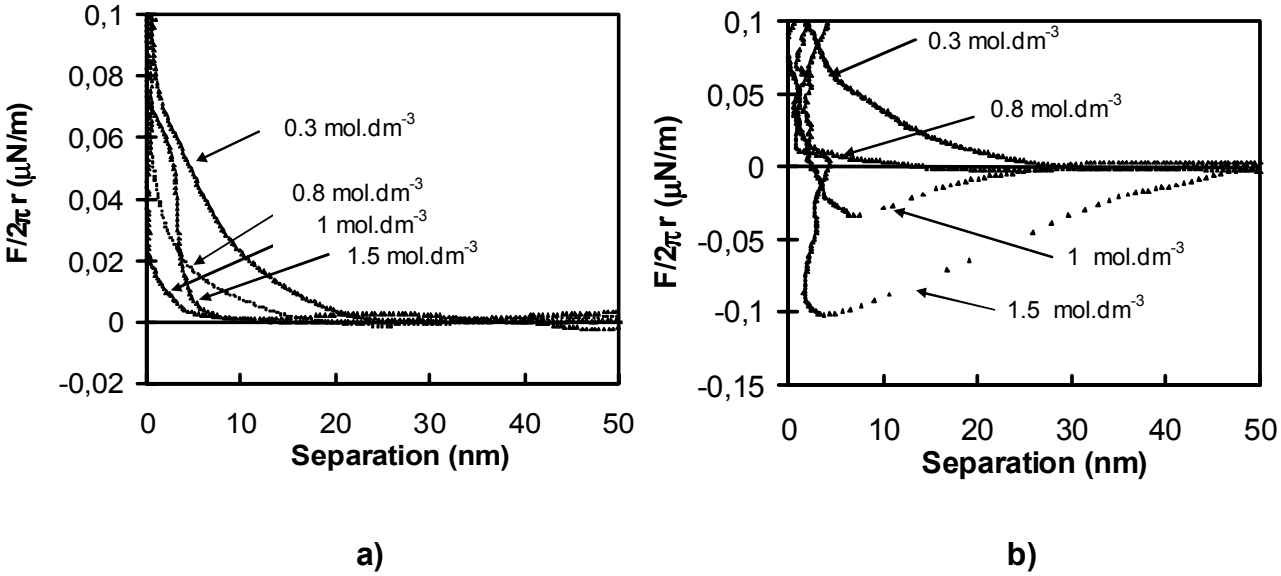

Figure 5

5: Figure 6

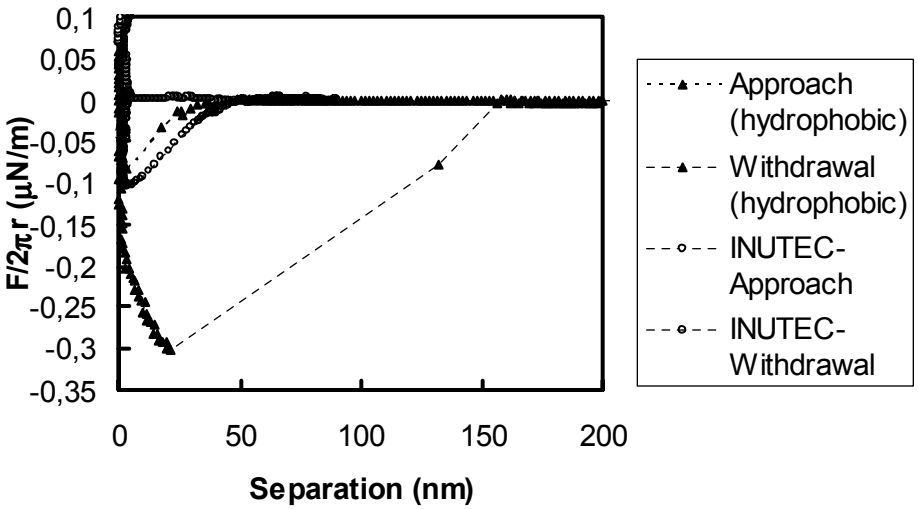

Figure 6

5: Figure 7

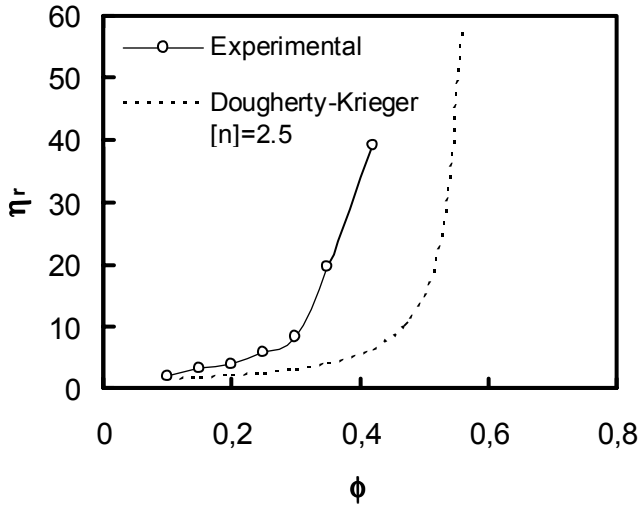

Figure 7